Letters in Applied NanoBioScience
Open-Access Journal (ISSN: 2284-6808)

Article
Volume 14, Issue 1, 2025, 1
https://doi.org/10.33263/LIANBS141.001

Antibacterial, Antioxidant, and Antidiabetic Activities of TiO_2 Nanoparticles Synthesized Through Ultrasonication Assisted Cold Maceration from Stem Extract of *Euphorbia hirta*

Vishwajeet Bachhar [1], Vibha Joshi [1], Ajay Singh [2,*], M. Amin Mir [3], Abhishek Bhardwaj [4]

[1] Department of Chemistry, DIT University, Dehradun, -248009 Uttarakhand
[2] Department of Chemistry, School of Applied and Life Sciences, Uttaranchal University, Dehradun
[3] Department of Mathematics and Natural Sciences, Prince Mohammad Bin Fahd University, AlKhobar, Saudi Arabia
[4] School of Pharmaceutical Sciences, Himgiri Zee University, Dehradun
* Correspondence: ajay21singh@yahoo.com;

Scopus Author ID 57212846073
Received: 23.11.2023; Accepted: 12.05.2024; Published: 21.09.2024

Abstract: The global scientific community recognizes the green synthesis of nanoparticles due to its environment-friendly approach. In this study, titanium dioxide nanoparticles(TiO_2 NPs) have been synthesized by ultrasonication-assisted cold maceration green technique mediated through stem extract of *Euphorbia hirta* such that the plant's phytochemical constituents are preserved and do not deteriorate. The synthesized TiO_2 nanoparticles were characterized by UV spectroscopy, and a sharp peak at 326 nm confirmed the formation of the TiO_2 nanoparticles. The surface morphology was analyzed using SEM (Scanning Electron Microscope), which showed that nanoparticles with flakes-like shapes were formed. EDX (Energy Dispersive X-ray Analysis) outcomes have also confirmed the presence of TiO_2. The antibacterial activity of the TiO_2 nanoparticles was assessed against three bacterial strains (Escherichia coli, Bacillus subtilis, and Pseudomonas aeruginosa.), with a maximum ZOI of 35±3.5 mm showing that TiO_2 nanoparticles have good antibacterial properties. Further antioxidant (DPPH and Phosphomolybdate assay) and antidiabetic activity were evaluated with the IC50 value of 39.01 ± 0.56, 48.29 ± 0.69, and 55 ± 1.69 µg/ml, respectively, which indicated the potency of the synthesized nanoparticles for various biomedical and pharmacological applications.

Keywords: *Euphorbia hirta*; nanoparticles; TiO_2; antibacterial; antioxidant; antidiabetic activity; cold maceration.

1. Introduction

With more than 1600 species, Euphorbia is the biggest genus in the Euphorbiaceae family. It may be recognized by the white, milky latex it generates, which is almost always fatal. The Euphorbia species *E. ingens*, *E. tirucalli*, and *E. may* have rubber in their lattices. This category of plants contains unique substances that have been identified, such as important secondary metabolites shown in Figure 1 [1–5]. It is a weed that originally came from the tropical regions of America and is also known as an asthma herb [6]. It is conveniently located in a few countries' marginally hotter regions, including Bangladesh, India, and Australia. It blooms openly around walkways, parks, drainages, and in the spaces between grasses. Traditional medicine uses this herb.

The field of nanotechnology is now advancing quickly [7]. Nanoparticle production is rapidly rising, and they are employed in a wide range of products, including antimicrobial creams, cosmetics, electrical devices, detectors, and medicine delivery systems in the body [8]. TiO_2 is being produced in large quantities globally for use in numerous fields [9]. Its distinct physical and chemical characteristics from those of typical powdered particles may affect the body's metabolism and other functions. The respiratory systems are significantly impacted by nanoparticles [10]. The pulmonary lungs and gastrointestinal tracts can both potentially absorb titanium nanoparticles. The mouth is the primary route via which titanium dioxide nanoparticles are administered orally [11]. In the realm of nanotechnology, nanomedicines are administered through direct injection into the veins, putting nanoparticles into the body's bloodstream [12]. Nanoparticles are also employed in a variety of therapies. For example, titanium dioxide is inhibited from working when coated with nanomaterials. Because of its color and high refractive index, titanium dioxide, a colored pigment, is the most widely used pigment in the world [13]. It has several uses, including non-stick coatings, food-related plastics, nanomedicine, and more. It is also photo-catalytically active and anticorrosive [14].

Euphorbia hirta is commonly used to treat gastrointestinal conditions such as intestinal parasitosis, diarrhea, dysentery, and respiratory problems like asthma and bronchitis. Other plant parts are also used to treat a variety of other diseases. Its leaflets can also be used to treat boils or swells. The anticancer and anti-inflammatory effects of the plant extract in combination with other metals have been astounding. This plant's ethanolic extract has demonstrated antibacterial action.

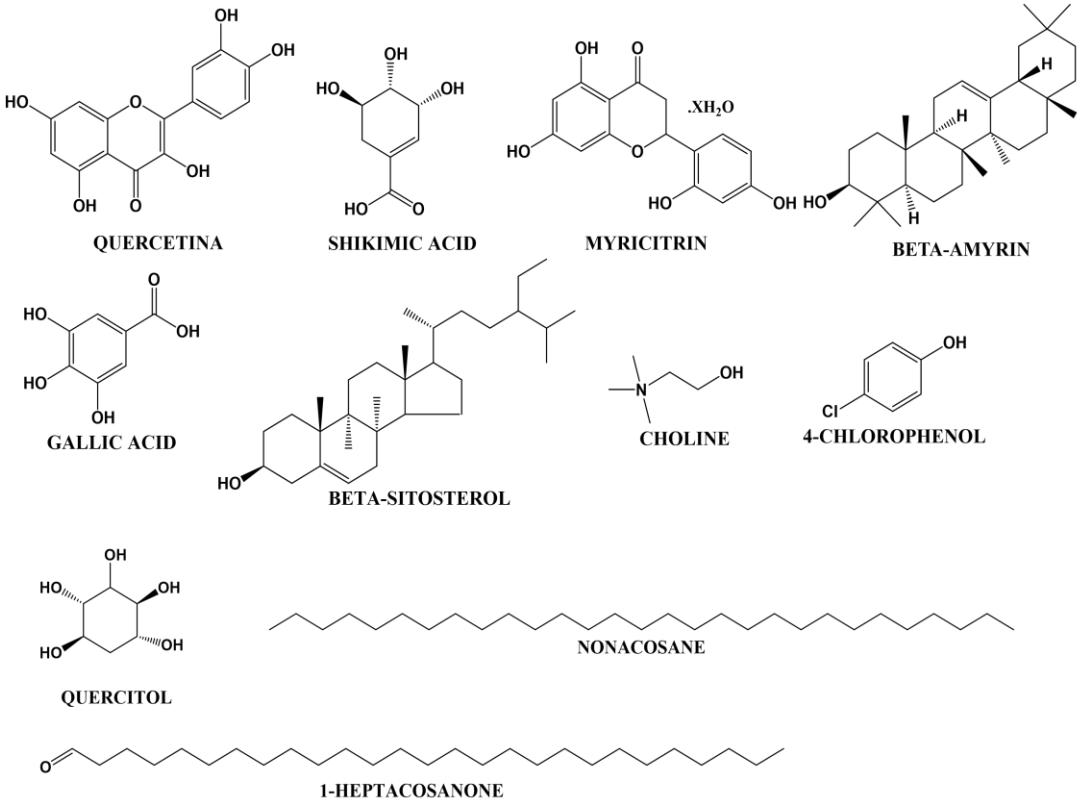

Figure 1. Chemical constituents of *E. hirta*.

Dry plant powder is also employed for skin conditions. It is additionally applied to snake bites [15]. It also demonstrated the anti-diarrheal effects at the dose of 55 mg per kg against the oil and acids and some other compounds induced diarrhea in the rat [16], and this showed the symptoms of diarrhea which was induced by the oil, some acids, and flavonoids

which were extracted from this plant. It also shows galactogenic activity by enhancing mammary gland development and increasing secretion; the finely ground powder of the plant has shown galactogenic activity in various pig breeds before the juvenile phase [17]. This plant's extracts are thought to treat female infertility and keep male sperm counts healthy [18].

The goal of this study is to prepare extract by ultrasonication-assisted cold maceration for the synthesis of TiO_2 nanoparticles from the stem extract of *Euphorbia hirta* and to evaluate its antibacterial, antioxidant (DPPH and Phosphomolybdate assay) and antidiabetic (Alpha-amylase assay) efficacy. The features of the plant and the titanium dioxide nanoparticle may coexist in the nanofabricated particles to produce better outcomes and more useful applications because the plant is biologically potent and has many health benefits. According to the literature review, no research on synthesizing titanium dioxide nanoparticles and its in-vitro phytochemical evaluation, antibacterial, antioxidant, and antidiabetic activity has been done in India's Kumaon region in Uttarakhand.

2. Materials and Methods

2.1. Materials.

Plant specimen was procured from Dineshpur, Uttarakhand, near August, and the fresh stem of *Euphorbia hirta* was harvested (Lattitude:29.0520046; Longitude:79.3211968). All the samples were handpicked. It is an erect, pubescent plant between 20 and 35 centimeters long. The leaves are 1-1.5 cm, widely oblong to elliptic-lanceolate, with an obliquely truncated base, serrulate border, and an acute, hispid tip. The petiole is up to 3 millimeters long.

2.2. Methods.

2.2.1. Preparation of extract.

To remove the dust sticking to the stem's surfaces, they were carefully cleaned with tap water and then rinsed with deionized water. The cleaned samples were dried under a running fan in a dimly lit area. After drying, the samples were ground into a coarse powder. 50 g powder was then kept in a conical flask with 200 ml ethanol and covered tightly with aluminum foil. After 7 days, the conical flask was placed in an ultrasonication machine for 18 hours, maintaining a constant temperature of 28°C. Then, the solution was filtered out, and the excess solvent was recovered using a rotary vacuum evaporator. For later usage, the extract was dried and kept in a vial at 4°C.

2.2.2. Green synthesis of nanoparticle.

In a 250 ml conical flask, 1.0 M of $TiCl_4$ solution was mixed in 100 ml distilled water. To this solution, 20 ml of freshly prepared extract was added, and then it was stirred for 2 hours at 25°C using a magnetic stirrer at 2000±100 RPM. There was a noticeable color change. The greenish color changed to a dark brown hue, which indicates that the plant extract has successfully reduced the precursor [19–22]. The reduced nanoparticles are centrifuged at 8000 RPM for 30 minutes. The clearly discernible solid residue was thoroughly cleaned with water three times and finally washed with ethanol. It was kept in a vacuum oven at 80°C for 24 hours for drying and then collected in vials for further characterization and biological screening.

2.2.3. Preliminary phytochemical screening.

Preliminary phytochemical screening of the extract is carried out by following the procedure by Bachhar *et al*. [23,24].

2.2.3.1. Test for steroids.

Liebermann-Burchard's test- Before filtering, the 0.5 g extract was diluted in 10 ml of anhydrous chloroform. The outcome was equally divided in half for the subsequent test. After combining the first portion of the solution with 1 ml of acetic anhydride, 1 ml of concentrated sulfuric acid was poured down the test tube's side to create a layer. The test tube was examined for any indication of steroid use, such as any green color.

2.2.3.2. Phenolics.

$FeCl_3$ test– 1 ml of extract was mixed with 2 ml of a 5% neutral $FeCl_3$ solution to determine the presence of phenolic compounds and tannins.

2.2.3.3. Terpenoids.

Horizon test– 2 ml of trichloroacetic acid was added to 1 ml of the extract. Terpenoids may be present, as demonstrated by the appearance of red precipitates.

2.2.3.4. Alkaloids.

Dragendroff's test- Dragendroff's reagent was added to plant extract in a test tube, and the precipitate's growth was watched for any indications of alkaloids' presence.

2.2.3.5. Proteins.

Million test- 3 ml of extract and 5 ml of Million's reagent were mixed together in a test tube. A curdy white precipitation formed, which, when heated, turned brick red. It may indicate the presence of amino acids.

2.2.3.6. Carbohydrates.

Molisch's test- A test tube with filtrate from the extract was filled with two drops of an alcoholic alpha-naphthol solution and 2 ml of concentrated sulfuric acid that had been carefully put along the test tube walls from another test tube. The formation of a purple ring at the junction indicates the presence of carbohydrates.

2.2.4. Characterization of nanoparticles.

The UV visible spectrophotometer (Shimadzu UV-1800 Japan) was used to analyze the confirmation of the formation of the TiO_2 nanoparticles; it was recorded in the range of 200-800 nm. The crystallinity and formation of the nanoparticles were determined by using X-ray diffraction (Rigaku). The surface morphology was investigated using a scanning electron microscope (Carl Zeiss Evo 18), and the SEM was already equipped with the software to measure the size of nanoparticles. EDX was used to quantify the elemental analysis, and the spectrum was used to determine the homogeneity and to determine the elemental distribution of the sample. The antibacterial activity of the TiO_2 nanoparticles was studied in 3 strains of bacteria using the disk diffusion method. Two techniques were used to evaluate antioxidant activity: the DPPH and phosphomolybdate assay. Alpha amylase inhibitory assay was used to

measure antidiabetic activity. The absorbance of the assays was recorded by using a digital spectrophotometer.

2.2.5. Antibacterial activity.

By using the disc diffusion technique, the antibacterial activity of *E. hirta* TiO_2 nanoparticles was evaluated. The stoppage of bacterial growth was left overnight. *Pseudomonas aeruginosa, Escherichia coli, and Bacillus subtilis* were the microorganisms employed in this assay. Using Whatman filter papers, which were cut into small, circular discs with a 6mm diameter, the strains were daubed in Agar. The solutions were formed with 3 concentrations, i.e., 20% (200 µg/ml), 40% (400 µg/ml), and 60% (600 µg/ml). Amoxicillin was used as standard at a concentration of (600 µg/ml). The paper discs and plates were autoclaved and sterilized. The disc was then coated with a nanoparticle of TiO_2, and the bacterial culture was incubated in the incubator at 38°C for around 24 hours. The outcomes were very excellent. The bacteria's growth was inhibited with dignity using an extremely accurate scale, and the average length of the suppression by each concentration was determined and indicated in millimeters, as shown in the results section.

2.2.6. Antioxidant activity.

2.2.6.1. DPPH assay.

The synthesized nanoparticles' antioxidant activity was evaluated using the digital spectrophotometer, opting for the method used by Santhoshkumar *et al*. [25,26]. In short, a 0.3 mM ethanol-based DPPH solution was made. The absorbance of DPPH in ethanol was measured at 517 nm as a control, and it remained constant during the test. 1ml ethanol was added in 3 sets of test tubes; in each of the test tubes, different concentrations, i.e., 20, 40, 60, 80, and 100 µl of the NPs solution were added. Later, 1 ml DPPH was added to this solution, and the test tubes were covered with the foil and kept in a dark room for 1 hour. The antioxidant activity was expressed as a percentage of radical scavenging activity and was calculated by the following formula:

$$RSA\ (\%) = 100\frac{(Ac-As)}{Ac} \qquad (1)$$

where *Ac* represented the control's absorbance (no nanoparticles) and *As* stood for the absorbance of the sample.

2.2.6.2. Phosphomolybdate assay.

The methodology opted for by Sujatha *et al*. [27] was used for the antioxidant efficacy of TiO2 nanoparticles, which was evaluated using the phosphomolybdate method. Test tubes were filled with samples (20, 40, 60, 80, and 100 µl) and 1 ml of the reagent solution (0.6 Molar sulfuric acid, 28 millimolar sodium phosphate, and 4 millimolar ammonium molybdate). After securely capping the test tubes with the foil, they were placed in a water bath at 95 °C for 90 minutes. After bringing the samples down to room temperature, the absorbance at 695 nm was determined. The standard was ascorbic acid. The calculation of antioxidant activity was done by using the following formula:

$$\%\ Inhibition = 100\ \frac{(Ac-As)}{Ac} \qquad (2)$$

where Ac represented the control's absorbance (no nanoparticles) and *As* stood for the absorbance of the sample.

2.2.7. Antidiabetic activity.

According to the methodology opted by Paun *et al*. [28,29], the antidiabetic potential was evaluated. One milliliter of reagent (0.20 mM phosphate buffer, pH 6.9) containing α-amylase (0.5 mg/ml)) solution was mixed with 20, 40, 60, 80, and 100 µl of test samples and standard medicine. The mixture was then incubated at 35°C for ten minutes. Following this, each test tube had 1 milliliter of a 1% starch solution in 0.02 Molar sodium phosphate buffer (pH 6.9). After that, the reaction mixtures were incubated for ten minutes at 35°C. A 1.0 milliliter DNS reagent was used to end the reaction. After five minutes of incubation in a boiling water bath, the test tubes were eventually allowed to cool to room temperature. After adding 5 ml of distilled water, the reaction mixture was diluted, and the absorbance at 540 nm was determined. For control, the experiment was conducted similarly by replacing nanoparticles with ethanol. Acarbose was used as standard. Plotting a percentage of α-amylase inhibition versus the concentration of TiO_2 nanoparticles allowed for calculating the IC_{50} values from the graph. The following is how the α-amylase inhibitory activity was determined:

$$\text{Inhibition (\%)} = \left(1 - \frac{As}{Ac}\right) X100 \qquad (3)$$

where *Ac* represented the control's absorbance (no nanoparticles) and *As* stood for the absorbance of the sample.

2.2.8. Statistical analysis.

Calculations and graphs were produced using MS Excel and Origin 9 Pro. All the experiments are repeated 3 times and are presented in the form of mean ± standard deviation.

3. Result and Discussion

3.1. Phytochemical analysis.

The plant extract is employed as a potential replacement for a reducing agent because of the presence of numerous key bioactive components such as terpenoids, alkaloids, phenolics, and tannins. The results of the phytochemical screening examination of the ethanolic plant extract are shown in Table 1. Alkaloids, flavonoids, sugars, and terpenoids are the plant's primary chemical constituents, as seen in Table 1. The outcomes of an in vitro phytochemical study are shown in Table 1.

Table 1. *In vitro* phytochemical screening.

S. No.	Bioactive chemicals	Results
1	Steroids	-
2	Phenolics	+
3	Terpenoids	+
4	Alkaloids	+
5	Proteins	+
6	Carbohydrates	+

(-) Represents absence and (+) represents presence

3.2. UV-visible spectral analysis.

The structural properties of TiO_2 nanoparticles were evaluated using a UV-visible spectrophotometer (Shimadzu UV-1800 Japan). 2 ml of TiO_2 NPs were introduced to the cuvette, and the calculation's "blank" was ethanol. Spectrum absorption of the TiO_2 NP was measured between 200 and 800 nm at various wavelengths. The resulting graph reveals that the sharp peak is at 326 nm in wavelength. A clear visual result with the absorption peak was shown after scanning. When the absorbance of the peak was compared with the absorbance of titanium dioxide nanoparticles using the sources, i.e., the internet and literature, the synthesized TiO_2 nanoparticles were validated [30,31]. When the particle size decreases, the adsorption edge will shift towards higher energy [32]. TiO_2 nanoparticle peak is depicted in Figure 1 by UV-visible spectrum analysis.

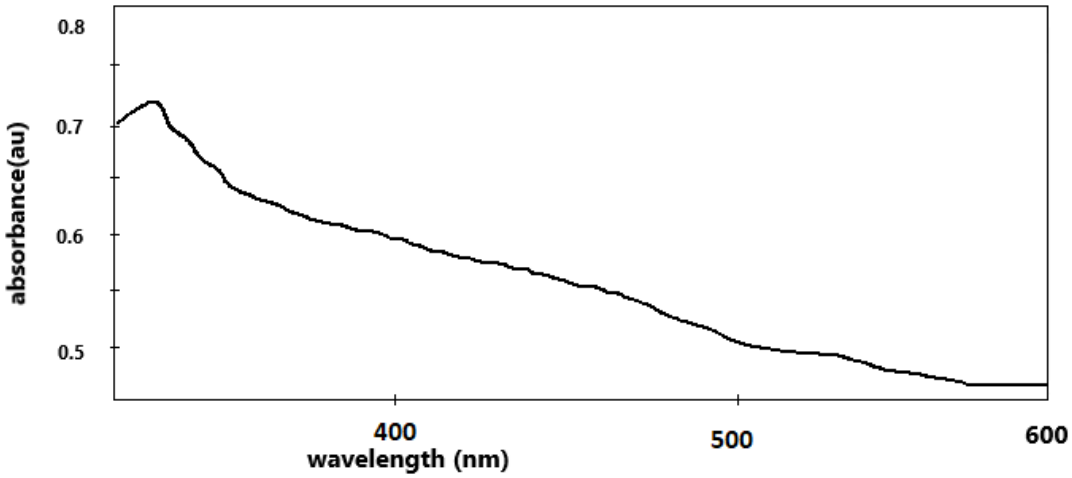

Figure 1. UV spectra of TiO_2 nanoparticles.

3.3. Scanning electron microscope (SEM).

The synthesized TiO_2 nanoparticles exhibited a flakes-like structure and aggregated into an irregular structure with an average diameter of 85 nm. It was discovered that the powder particles were rather tightly packed. TiO_2 nanoparticle composition was investigated using EDX analysis. Figure 2 depicts the surface morphology of TiO_2 nanoparticles. The powder particles were found to be quite densely packed. EDX analysis was used to study the composition of TiO_2 nanoparticles Figure 3. The surface morphology of TiO_2 nanoparticles is seen in the image below.

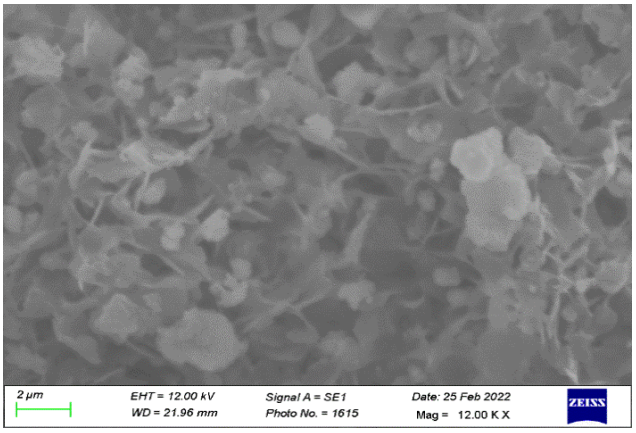

Figure 2. SEM image of TiO_2 nanoparticles.

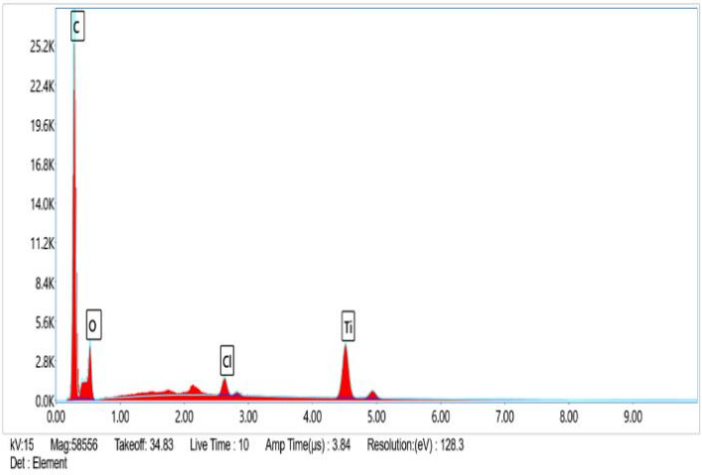

Figure 3. EDX report of TiO_2 nanoparticles.

Table 2. Percentage of constituent present in the nanoparticle.

eZAF Quant - Analysis Uncertainty: 99.00 %

Component	Weight %	Atomic %	Error %	Net Int.
C	68.3	80.6	8.8	45265.6
O	16.6	14.7	11.6	5768.3
Cl	1.7	0.7	4.1	1420.5
Ti	13.5	4.0	2.7	5645.7

3.4. XRD analysis.

X-ray diffraction of the nanoparticles was performed using a 40 kV X-ray source with cu and k radioactivity. In this study, the TiO_2 powder's size was reduced through the use of a physical grinding technique. With a mortar and pestle, about 10 mg of TiO_2 powder was crushed into a fine powder. It was consistently ground and finely powdered and was characterized by XRD. Data were gathered for the 2 range from an X-ray diffractometer examination of the synthesized sample of TiO_2 nanoparticles using Cu-K X-rays. The formation of TiO_2 nanoparticles was validated by the study's peak results of XRD with the reported one. The XRD pattern is shown in Figure 4. The anatase phase of TiO2 is confirmed by all of the diffraction peaks cited at 24.310 (101), 37.79 (004), 48.050 (200), 53.889 (105), and 68.761 (116) in the XRD pattern of the synthesized TiO_2 NPs, which correlates with the JCPDS database (89–4921) [33].

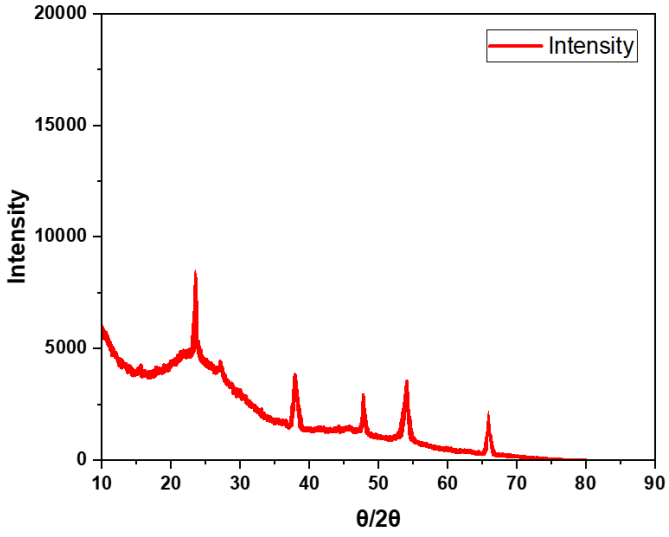

Figure 4. XRD Spectra of TiO_2 nanoparticles.

3.5. Antibacterial activity.

TiO_2 nanoparticles have shown excellent effectiveness against three types of bacteria: *Escherichia coli, Bacillus subtilis, and Pseudomonas aeruginosa.* It was discovered that the plant-mediated TiO_2 nanoparticles have extremely substantial antibacterial activity against *Escherichia coli* (37 ± 3.4mm), *Pseudomonas aeruginosa* (35 ± 3.5 mm), and *Bacillus subtilis* (36 ± 2.3 mm) against the standard amoxicillin wiz. (23 ± 2.2 mm), (22 ± 1.5 mm) (15 ± 1.44 mm), respectively, at the maximum concentration of 600 µg/ml as shown in Figures 5 and 6. The experiment was done in triplicate. Disc diffusion analyses are performed to recognize ZOI, a circular appearance formed in the Petri dish, which a ruler then measures. The titanium dioxide nanoparticles are capable of inhibiting bacterial growth by dissolving the outer membrane of the bacteria. The study's findings indicate that the nanoparticles outperform regular amoxicillin in terms of effectiveness.

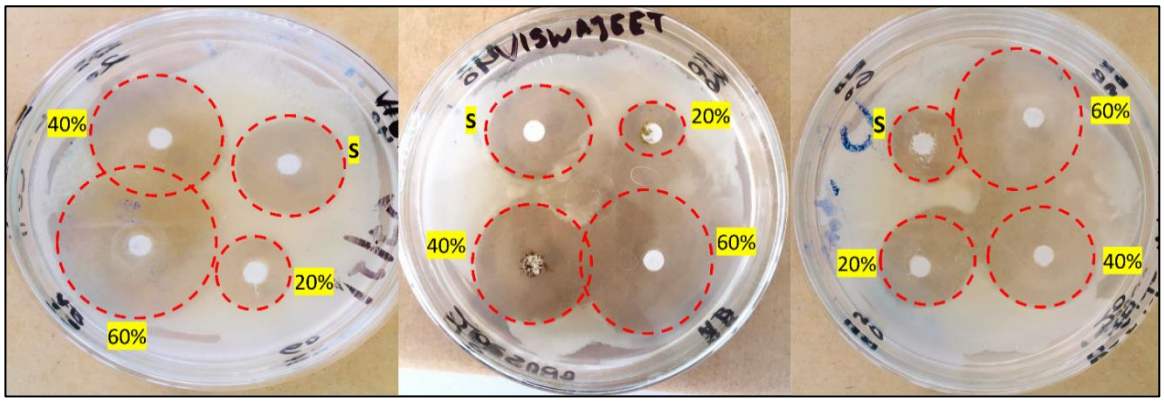

(a) **(b)** **(c)**

Figure 5. Zone of inhibitions of **(a)** *Escherichia coli*; **(b)** *Pseudomonas aeruginosa*; **(c)** *Bacillus subtilis*, and the standard is shown by S.

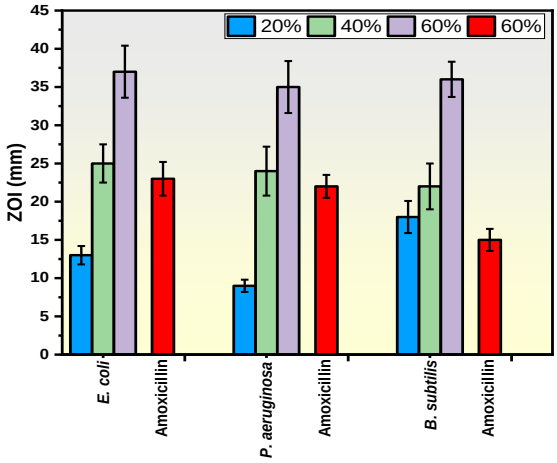

Figure 6. Shows the zone of inhibition of the bacteria compared with the standard amoxicillin.

3.6. Antioxidant activity.

The antioxidant activity of synthesized TiO_2 nanoparticles made from *Euphorbia hirta* stem extract was assessed in this work, and it was discovered that they were potent antioxidants. When the nanoparticle concentration is increased from 20 to 100 µl, a noticeable color shift is seen in the phosphomolybdate and DPPH tests. The color shift, which indicates the nanoparticle's potential for reduction, suggests that the sample may be a strong antioxidant. Figure 7 displays the ascorbic acid (as standard) and TiO_2 nanoparticle's DPPH radical

scavenging abilities. The DPPH radical scavenging activity of TiO_2 nanoparticles was good, with an IC_{50} value of 39.01 ± 0.56 µg/ml. This result, at 25.36 ± 1.02 µg/ml, was marginally higher than that of ascorbic acid. All samples showed DPPH radical scavenging activity in a dose-dependent manner. The same dose-dependent action has also been seen in the phosphomolybdate assay, as the antioxidant capacity increases with the increase in the concentration of the nanoparticles. The calculated IC_{50} value for phosphomolybdate assay was 48.29 ± 0.69µg/ml, and for standard ascorbic acid, it was found to be 34.07 ± 0.39µg/ml. Figure 7 depicts the comparison of IC_{50} of two methods with standard. Based on the results, the domains of pharmacology and biology can make use of these nanoparticles.

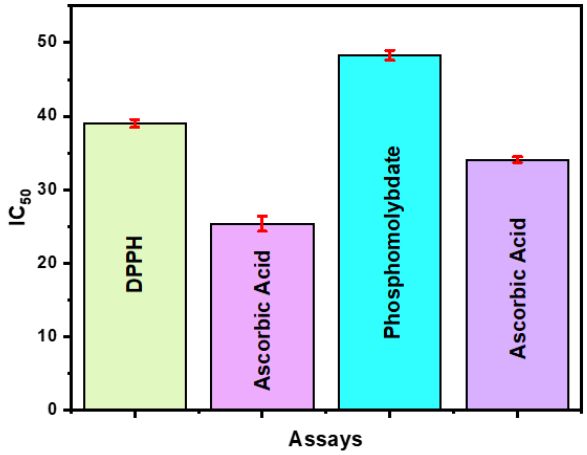

Figure 7. Shows IC_{50} DPPH and Phosphomolybdate Assay compared with the standard.

3.7. Antidiabetic activity.

An essential enzyme in the metabolism of carbohydrates is α -amylase. One of the greatest methods to lower blood sugar is to inhibit α-amylase. Starch blockers, also known as amylase inhibitors, stop the body from absorbing starches from food. Therefore, it will lessen the typical spike in blood sugar caused by carbohydrate ingestion.

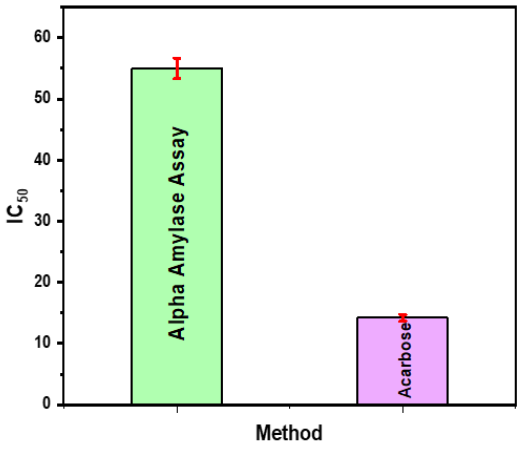

Figure 8. Shows IC_{50} of α-amylase assay compared with standard.

Treating diabetes will benefit more from using nanoparticles with strong antioxidant activity. The calculated IC_{50} value measured was 55 ± 1.69µg/ml, whereas the IC_{50} value of standard acarbose have 14.21 ± 0.53µg/ml, which depicts the good antidiabetic potential of the synthesized TiO_2 nanoparticles. Figure 8 shows the comparison between the IC_{50} value of the standard and synthesized nanoparticles.

From the outcomes of the activities, it can be concluded that the TiO_2 nanoparticles synthesized from the stem extract of *Euphorbia hirta* are very potent particles as they show good IC_{50} values. So, these particles can be used in various fields such as medical, pharmaceutical, and drug delivery systems.

4. Conclusions

Titanium dioxide nanoparticles have been successfully synthesized using the stem extract of *E. hirta* from northern India. According to the phytochemical screening test, the plant's ethanolic extract has a range of bioactive ingredients, including plant metabolites and other phytochemicals. The synthesis of titanium dioxide nanoparticles was verified by UV-visible spectroscopy. The absorbance peak indicates the presence of TiO_2 nanoparticles, XRD, and SEM, while the elemental composition of the nanoparticles was also tested through EDX. The antibacterial activity of *E. hirta* was tested using the disc diffusion method, and the findings are good compared to the performance of the standard antibiotic. Our analysis revealed that a significant amount of bacterial growth was suppressed at different nanoparticle concentrations. From the antioxidant activity, it is concluded that the nanoparticles have an excellent free radical quenching property. The alpha-amylase inhibitory activity showed good antidiabetic properties in these nanoparticles. Further, the TiO_2 nanoparticles can be explored for many other biological in-vivo activities to analyze their efficiency and for drug discovery.

Funding

This research received no external funding.

Acknowledgments

Declared none.

Conflict of Interest

The authors declare no conflict of interest.

References

1. Kumar, S.; Malhotra, R.; Kumar, D. Euphorbia Hirta: Its Chemistry, Traditional and Medicinal uses, and Pharmacological Activities. *Pharmacogn. Rev.* **2010**, *4*, 58–61, https://dx.doi.org/10.4103/0973-7847.65327.
2. Nuryanti, A.; Sarasati, A.; Ulfahastika, L.; Wartadiani, M.D.; Syahruddin, M.H.; A'Yun, R.N.S.Q. *Euphorbia hirta* nanoextract as a piezoelectric ultrasonic scaler coolant in gingivitis treatment in a Wistar rat model. *J. Taibah Univ. Med. Sci.* **2024**, *19*, 1–9, https://doi.org/10.1016/j.jtumed.2023.09.004.
3. Meda, R.N.-T.; Kam, S.E.; Kagambega, W.; Zongo, E.; Ouedraogo, C.; Segda, A.; Koama, B.K.; Somda, F.T.; Zongo, E.; Ouedraogo, G.A. A Review on Bioactive Compounds Isolated from *Euphorbia hirta* L. *Am. J. Plant Sci.* **2023**, *14*, 710–726, https://doi.org/10.4236/ajps.2023.146048.
4. Shwetha, S.; Ramesh, C.; Pinkey, R.; Sowmya, B.A.; Maria, L.A.; Ranjitha, C.J. The ethanol extract of Euphorbia hirta exhibits in vitro antidiabetic potentials by sensitization of the insulin. *J. Drug Deliv. Ther.* **2023**, *13*, 125–127, https://doi.org/10.22270/jddt.v13i9.6209.
5. Chapeta, A.C.O.; Tozin, L.R.d.S.; Souza, A.d.S.; Costa, M.G.; Leal, J.F.L.; Pinho, C.F.d. Leaf and stem anatomical characterization of *Euphorbia hirta* L., a tolerant species to glyphosate. *J. Environ. Sci. Health - B* **2023**, *58*, 203–209, https://doi.org/10.1080/03601234.2023.2177462.
6. Das, K.; Asdaq, S.M.B.; Khan, M.S.; Amrutha, S.; Alamri, A.; Alhomrani, M.; Alsanie, W.F.; Bhaskar, A.; Chandana shree, G.; Harshitha, P. Phytochemical investigation and evaluation of *in vitro* anti-inflammatory

activity of *Euphorbia hirta* ethanol leaf and root extracts: A comparative study. *J King Saud Univ. Sci*. **2022**, *34*, 102261, https://doi.org/10.1016/j.jksus.2022.102261.
7. Roco, M.C. The long view of nanotechnology development: the National Nanotechnology Initiative at 10 years. *J. Nanopart. Res.* **2011**, *13*, 427–445, https://doi.org/10.1007/s11051-010-0192-z.
8. Jaiswal, K.K.; Kumar, V.; Vlaskin, M.S.; Sharma, N.; Rautela, I.; Nanda, M.; Arora, N.; Singh, A.; Chauhan, P.K. Microalgae fuel cell for wastewater treatment: Recent advances and challenges. *J. Water Process Eng.* **2020**, *38*, 101549, https://doi.org/10.1016/j.jwpe.2020.101549.
9. Shi, H.; Magaye, R.; Castranova, V.; Zhao, J. Titanium dioxide nanoparticles: a review of current toxicological data. *Part. Fibre Toxicol.* **2013**, *10*, 15, https://doi.org/10.1186/1743-8977-10-15.
10. Lu, X.; Zhu, T.; Chen, C.; Liu, Y. Right or Left: The Role of Nanoparticles in Pulmonary Diseases. *Int. J. Mol. Sci.* **2014**, *15*, 17577–17600, https://doi.org/10.3390/ijms151017577.
11. Mortensen, N.P.; Pathmasiri, W.; Snyder, R.W.; Caffaro, M.M.; Watson, S.L.; Patel, P.R.; Beeravalli, L.; Prattipati, S.; Aravamudhan, S.; Sumner, S.J.; Fennell, T.R. Oral administration of TiO_2 nanoparticles during early life impacts cardiac and neurobehavioral performance and metabolite profile in an age- and sex-related manner. *Part. Fibre Toxicol.* **2022**, *19*, 3, https://doi.org/10.1186/s12989-021-00444-9.
12. Narum, S.M.; Le, T.; Le, D.P.; Lee, J.C.; Donahue, N.D.; Yang, W.; Wilhelm, S. Chapter 4 - Passive targeting in nanomedicine: fundamental concepts, body interactions, and clinical potential. In Nanoparticles for Biomedical Applications, Chung, E.J., Leon, L., Rinaldi, C., Eds.; Elsevier, **2019**; 37–53, https://doi.org/10.1016/B978-0-12-816662-8.00004-7.
13. Gázquez, M.J.; Bolívar, J.P.; García-Tenorio García-Balmaseda, R.; Vaca, F. A Review of the Production Cycle of Titanium Dioxide Pigment. *Mater. Sci. Appl.* **2014**, *5*, 441–458, https://doi.org/10.4236/msa.2014.57048.
14. Iesalnieks, M.; Eglītis, R.; Juhna, T.; Šmits, K.; Šutka, A. Photocatalytic Activity of TiO2 Coatings Obtained at Room Temperature on a Polymethyl Methacrylate Substrate. *Int. J. Mol. Sci.* **2022**, *23*, 12936, https://doi.org/10.3390/ijms232112936.
15. Uddin, M.S.; Billah, M.M.; Nahar, Z. Pharmacological actions of *Euphorbia hirta*: A review. *Int. J. Hortic. Food Sci.* **2019**, *1*, 84–89, https://doi.org/10.33545/26631067.2019.v1.i1b.17.
16. Brijesh, S.; Daswani, P.G.; Tetali, P.; Rojatkar, S.R.; Antia, N.H.; Birdi, T.J. Studies on *Pongamia pinnata* (L.) Pierre leaves: understanding the mechanism(s) of action in infectious diarrhea. *J. Zhejiang Univ. Sci. B* **2006**, *7*, 665–674, https://doi.org/10.1631/jzus.2006.B0665.
17. Koko, B.K.; Konan, A.B.; Kouacou, F.K.A.; Djétouan, J.M.K.; Amonkan, A.K. Galactagogue effect of *Euphorbia hirta* (Euphorbiaceae) aqueous leaf extract on milk production in female wistar rats. *J. Biosci. Med.* **2019**, *7*, 51–65, https://doi.org/10.4236/jbm.2019.79006.
18. Oguejiofor, C.F.; Onyejekwe, O.B.; Onwuzurike, O.I. *In vitro* immobilizing and spermicidal effects of methanol leaf extract of *Euphorbia hirta* Linn. (Euphorbiaceae) on caprine spermatozoa. *Trop. J. Pharm. Res.* **2021**, *20*, 329–336, https://doi.org/10.4314/tjpr.v20i2.16.
19. Nagalingam, M.; Kalpana, V.N.; Devi Rajeswari, V.; Panneerselvam, A. Biosynthesis, characterization, and evaluation of bioactivities of leaf extract-mediated biocompatible gold nanoparticles from *Alternanthera bettzickiana*. *Biotechnol. Rep.* **2018**, *19*, e00268, https://doi.org/10.1016/j.btre.2018.e00268.
20. Jaffar, S.S.; Saallah, S.; Misson, M.; Siddiquee, S.; Roslan, J.; Lenggoro, W. Green Synthesis of Flower-Like Carrageenan-Silver Nanoparticles and Elucidation of Its Physicochemical and Antibacterial Properties. *Molecules* **2023**, *28*, 907, https://doi.org/10.3390/molecules28020907.
21. Azwatul, H.M.; Uda, M.N.A.; Gopinath, S.C.B.; Arsat, Z.A.; Abdullah, F.; Muttalib, M.F.A.; Hashim, M.K.R.; Hashim, U.; Isa, M.; Uda, M.N.A.; Radi Wan Yaakub, A.; Ibrahim, N.H.; Parmin, N.A.; Adam, T. Plant-based green synthesis of silver nanoparticle via chemical bonding analysis. *Mater. Today Proc.* **2023**, https://doi.org/10.1016/j.matpr.2023.01.005.
22. Takcı, D.K.; Ozdenefe, M.S.; Genc, S. Green synthesis of silver nanoparticles with an antibacterial activity using *Salvia officinalis* aqueous extract. *J. Cryst. Growth* **2023**, *614*, 127239, https://doi.org/10.1016/j.jcrysgro.2023.127239.
23. Bachhar, V.; Joshi, V.; Gangal, A.; Duseja, M.; Shukla, R.K. Identification of Bioactive Phytoconstituents, Nutritional Composition and Antioxidant Activity of *Calyptocarpus vialis*. *Appl. Biochem. Biotechnol.* **2024**, *196*, 1921-1947, https://doi.org/10.1007/s12010-023-04640-5.
24. Joshi, J.; Bachhar, V.; Singh, A.; Duseja, M. Green Synthesis of TiO_2 Nanoparticles Using Root Extract of *Asparagus racemosus* (Shatavari) and Evaluation of Its Antibacterial, Antioxidant and Antidiabetic activities. *Med. Anal. Chem. Int. J.* **2023**, *7*, 000184, https://doi.org/10.23880/macij-16000184.

25. Santhoshkumar, T.; Rahuman, A.A.; Jayaseelan, C.; Rajakumar, G.; Marimuthu, S.; Kirthi, A.V.; Velayutham, K.; Thomas, J.; Venkatesan, J.; Kim, S.-K. Green synthesis of titanium dioxide nanoparticles using *Psidium guajava* extract and its antibacterial and antioxidant properties. *Asian Pac. J. Trop. Med.* **2014**, *7*, 968–976, https://doi.org/10.1016/S1995-7645(14)60171-1.
26. Gulcin, İ.; Alwasel, S.H. DPPH Radical Scavenging Assay. *Processes* **2023**, *11*, 2248, https://doi.org/10.3390/pr11082248.
27. Sujatha, S.; Sekar, T. FREE-RADICAL SCAVANGING ACTITIVTY LEAF EXTRACT OF LITSEA LAEVIGATA GAMBLE. *Int. J. Pharm. Pharm. Sci.* **2019**, *11*, 96–103, https://doi.org/10.22159/ijpps.2019v11i3.30594.
28. Paun, G.; Neagu, E.; Albu, C.; Savin, S.; Radu, G.L. *In Vitro* Evaluation of Antidiabetic and Anti-Inflammatory Activities of Polyphenolic-Rich Extracts from *Anchusa officinalis* and *Melilotus officinalis*. *ACS Omega* **2020**, *5*, 13014–13022, https://doi.org/10.1021/acsomega.0c00929.
29. Jaber, S.A. *In vitro* alpha-amylase and alpha-glucosidase inhibitory activity and *in vivo* antidiabetic activity of *Quercus coccifera* (Oak tree) leaves extracts. *Saudi J. Biol. Sci.* **2023**, *30*, 103688, https://doi.org/10.1016/j.sjbs.2023.103688.
30. Ngoepe, N.M.; Mathipa, M.M.; Hintsho-Mbita, N.C. Biosynthesis of titanium dioxide nanoparticles for the photodegradation of dyes and removal of bacteria. *Optik* **2020**, *224*, 165728, https://doi.org/10.1016/j.ijleo.2020.165728.
31. Singh, M.K.; Mehata, M.S. Phase-dependent optical and photocatalytic performance of synthesized titanium dioxide (TiO_2) nanoparticles. *Optik* **2019**, *193*, 163011, https://doi.org/10.1016/j.ijleo.2019.163011.
32. Li, D.; Song, H.; Meng, X.; Shen, T.; Sun, J.; Han, W.; Wang, X. Effects of Particle Size on the Structure and Photocatalytic Performance by Alkali-Treated TiO_2. *Nanomaterials* **2020**, *10*, 546, https://doi.org/10.3390/nano10030546.
33. Kalaiarasi, S.; Jose, M. Dielectric functionalities of anatase phase titanium dioxide nanocrystals synthesized using water-soluble complexes. *Appl. Phys. A Mater. Sci. Process.* **2017**, *123*, 512, https://doi.org/10.1007/s00339-017-1121-0.